

# DiFlowDubber: Discrete Flow Matching for Automated Video Dubbing via Cross-Modal Alignment and Synchronization

Ngoc-Son Nguyen<sup>1</sup> Thanh V. T. Tran<sup>1</sup> Jeongsoo Choi<sup>2</sup> Hieu-Nghia Huynh-Nguyen<sup>1\*</sup>  
 Truong-Son Hy<sup>3</sup> Van Nguyen<sup>1†</sup>  
<sup>1</sup>FPT Software AI Center, Vietnam <sup>2</sup>KAIST, South Korea  
<sup>3</sup>University of Alabama at Birmingham, USA

## Abstract

Video dubbing has broad applications in filmmaking, multimedia creation, and assistive speech technology. Existing approaches either train directly on limited dubbing datasets or adopt a two-stage pipeline that adapts pre-trained text-to-speech (TTS) models, which often struggle to produce expressive prosody, rich acoustic characteristics, and precise synchronization. To address these issues, we propose **DiFlowDubber** with a novel two-stage training framework that effectively transfers knowledge from a pre-trained TTS model to video-driven dubbing, with a discrete flow matching generative backbone. Specifically, we design a *FaPro* module that captures global prosody and stylistic cues from facial expressions and leverages this information to guide the modeling of subsequent speech attributes. To ensure precise speech-lip synchronization, we introduce a *Synchronizer* module that bridges the modality gap among text, video, and speech, thereby improving cross-modal alignment and generating speech that is temporally synchronized with lip movements. Experiments on two primary benchmark datasets demonstrate that *DiFlowDubber* outperforms previous methods across multiple metrics.

## 1. Introduction

Visual voice cloning (V2C), or video dubbing, generates speech conditioned on subtitle text, reference speech, and reference video, ensuring the target voice is preserved, lip-synchronized, and expressive of video-driven emotion. Despite notable advances in video dubbing [12–14, 64, 65], synthesized speech often falls short in overall quality, particularly in terms of naturalness, pronunciation accuracy, and synchronization. A primary bottleneck is the scarcity of large-scale legally shareable dubbing data, which is constrained by copyright issues. Meanwhile, modern TTS systems pre-trained in large-scale high-quality corpora [62]

\*Independent researcher, work done in part while author was at the FPT Software AI Center, Vietnam. †Corresponding author.

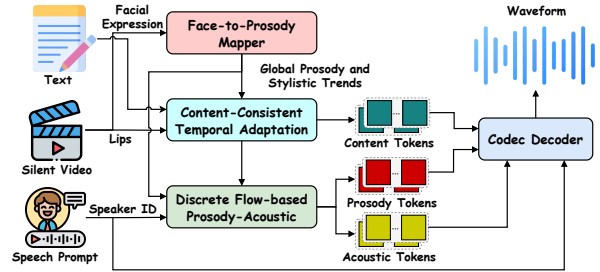


Figure 1. Overall inference pipeline of DiFlowDubber. The *Face-to-Prosody Mapper* module predicts global prosody priors that capture global prosody and stylistic cues from facial expressions. The *Content-Consistent Temporal Adaptation* module generates discrete content tokens conditioned on lip movements, text, and prosody priors, ensuring consistent with the target text transcription and temporal alignment. *Discrete Flow-based Prosody-Acoustic* module generates diverse yet globally consistent prosody tokens under the guidance of the prosody prior, together with corresponding acoustic tokens. The speech waveform is synthesized from the predicted tokens and speaker embedding via a Codec Decoder.

are capable of generating high-fidelity speech, yet they still lack video-conditioned affect and precise lip synchronization. A natural solution is to adapt pre-trained TTS models for video dubbing while preserving their original capabilities. Speaker2Dubber [64] attempts this approach by pre-training on a large TTS corpus and then adapting its phoneme encoder for the dubbing task. While this improves the richness of linguistic representations, it fails to fully leverage the advantages of large-scale TTS pre-training, such as prosody and acoustic modeling. To address this limitation, ProDubber [65] introduces a prosody-enhanced acoustic pre-training stage and an acoustic-prosody disentanglement stage to achieve higher-quality dubbing with better prosody alignment. However, this method primarily focuses on improving speech quality but still struggles with synchronization, as it relies on a duration predictor to estimate lip movements that are not constrained by the actual video length, resulting in poor audio-visual synchronization.

To address these issues, we present **DiFlowDubber**, a

novel approach for automated video dubbing based on Discrete Flow Matching (DFM) [19]. Our motivation is to design a framework that fully exploits the advantages of large-scale TTS pre-training, particularly in modeling prosody, content, and acoustic characteristics, and adapt it for video dubbing while preserving pronunciation accuracy, naturalness, and precise lip synchronization. To this end, we first employ a pre-trained FAcCodec [28] to decompose speech into prosody, content, and acoustic tokens, which serve as our target discrete representations. This choice is motivated by two key factors: (1) FAcCodec factorizes speech attributes such as prosody, content, and acoustic information, making them easier to control and model; and (2) it is pre-trained on a large-scale multi-speaker corpus, providing a strong and reliable codec foundation for our target data. Building on this representation, we design a novel two-stage pipeline:

**In the first stage**, we develop a zero-shot TTS system that models factorized speech representations to synthesize high-quality speech in a discrete setting. To this end, the system is pre-trained in a zero-shot TTS configuration, where we employ a simple deterministic content modeling architecture to efficiently capture linguistic structure. In contrast, for prosody and acoustic attributes, we adopt a generative modeling approach using discrete flow matching through the *Discrete Flow-Based Prosody-Acoustic* (DFPA) module to capture expressive prosodic variations and realistic acoustic diversity from the corpus. **In the second stage**, the pre-trained TTS model is adapted for video dubbing, as illustrated in Figure 1. To address the synchronization challenge during domain adaptation, we introduce the *Synchronizer*, which takes phoneme sequences and lips-cropped visual features as inputs to capture temporally aligned content details. In addition, we design the *Face-to-Prosody Mapper* (*FaPro*) module to extract global prosodic cues from face-cropped video frames. These features are fused with the synchronized content representation to construct a rich, fine-grained multimodal embedding that captures prosody-content correlations. Finally, this embedding, together with the global prosody features, is fed into the DFPA, which is initialized and fine-tuned from the pre-trained TTS model to generate diverse prosodic variations along with the corresponding acoustic tokens. We summarize our contributions as follows:

- We propose DiFlowDubber, an end-to-end automated video dubbing framework built upon a DFM generative backbone. Our approach consists of a zero-shot TTS pre-training stage that fully exploits content information, expressive prosodic variations, and realistic acoustic diversity from large-scale corpora, followed by a transfer learning stage that adapts the pretrained TTS model to visual inputs for video dubbing. To the best of our knowledge, this is the first work to extend DFM to video dubbing.
- We propose a novel *Synchronizer* module that effectively bridges the modality gap between text, video, and speech.

This module enhances video-speech alignment through a dual-alignment mechanism which collectively enforces robust cross-modal synchronization.

- Extensive experiments on two major benchmarks demonstrate that DiFlowDubber surpasses state-of-the-art (SOTA) baselines, achieving superior content accuracy, naturalness, and synchronization with video.

## 2. Related work

### 2.1. Speech synthesis

Speech synthesis has undergone rapid progress in recent years, moving from concatenative and statistical parametric approaches [26, 61] to deep generative models that achieve human-like naturalness. Early neural architectures [51, 57] demonstrated the feasibility of end-to-end TTS by jointly modeling prosody and waveform generation. Subsequent advances have focused on improving efficiency and controllability, with non-autoregressive models [31, 48, 50] reducing inference latency while maintaining quality. More recently, discrete representation learning [1, 4, 29, 46, 58] and diffusion/flow-based methods [6, 17, 20, 24, 28–34, 38, 41, 52] have further improved expressiveness and robustness, allowing fine-grained control over prosody, speaker identity, and style. Parallel to these developments, large language models have been integrated with TTS pipelines [3, 5, 18, 21, 22, 27, 39, 44, 53, 56, 63], bridging the gap between linguistic understanding and acoustic realization. Despite these advances, most systems remain text-driven, limiting their applicability in multimodal scenarios such as video dubbing, where visual articulatory cues are essential for precise synchronization. Building on these foundations, we extend discrete generative modeling to incorporate visual cues, addressing the modality gap between text-based TTS and video-conditioned speech synthesis.

### 2.2. Visual Voice Cloning

The V2C task requires the models to align the prosody and timing of generated speech with the input video to achieve automatic dubbing. Early efforts in V2C explored lip-to-speech generation [7, 45, 60], showing that visual articulatory cues provide strong constraints for intelligibility. More recent approaches have incorporated multimodal inputs, leveraging text and video to improve synchronization and naturalness. One line of work has emphasized hierarchical modeling, where prosodic features such as rhythm, intonation, and duration are jointly synchronized with facial expressions and contextual video dynamics [12]. Other approaches have focused on character-specific expressiveness: for example, StyleDubber [13] integrates phoneme-level details with emotion variation to reproduce distinctive speaking styles, while EmoDubber [14] leverages a flow-based design with emotion-aware conditioning to modulate intensity. Addressing pronunciation accuracy, Speaker2Dubber [64] pre-trains

its phoneme encoder on large-scale text-speech corpora to improve articulation. Among the most relevant for our study, ProDubber [65] adopts a two-phase training pipeline that transfers knowledge from extensive TTS datasets. However, ProDubber employs a duration predictor to upsample acoustic text features to the spectrogram length based on predicted alignments. Since this process is not constrained by the actual video length, it can lead to suboptimal lip-sync error (LSE) scores (see Tables 1 and 2).

### 3. Methodology

#### 3.1. Overview

Our framework is designed as an end-to-end pipeline. We first pre-train a zero-shot TTS system that learns to control and model complex speech attributes, including prosody, content, and acoustic characteristics. The content attribute is modeled as illustrated in Figure 2 (Teacher box), while the Discrete Flow-Based Prosody-Acoustic (DFPA) generates tokens that capture expressive prosody and realistic acoustic characteristics consistent with a given speech prompt (Figure 2b, orange arrow). We then adapt this pre-trained model to the movie dubbing domain, enabling it to inherit the advantages of the large-scale TTS corpus by integrating visual cues, as illustrated in Figure 1. This adaptation is achieved through two key components: (a) Content-Consistent Temporal Adaptation (CCTA) (Section 3.4.3), which transfers knowledge from the TTS domain to generate content representations consistent with the target text transcription, achieving precise lip synchronization and capturing captures global prosodic states conveyed through visual cues; and (b) DFPA modeling with modified conditioning to better suit the visual modality which is detailed in Section 3.4.4.

#### 3.2. Data Preparation

We detail the input representations of each modality.

**Discrete Speech Tokens.** We leverage the pre-trained FA-Codec [28], which consists of a Codec Encoder and a Codec Decoder. The encoder decomposes raw speech into *prosody*, *content*, and *acoustic* token sequences, which serve as our discrete target data, along with a *speaker identity* embedding. The decoder subsequently reconstructs the speech waveform from these tokens and the corresponding speaker identity.

Given a speech waveform  $\mathbf{S}$ , we apply the Codec Encoder to extract a sequence of discrete speech tokens along with a speaker embedding. This process yields  $\mathbf{x}_p \in \mathbb{R}^{m \times L}$ ,  $\mathbf{x}_c \in \mathbb{R}^{n \times L}$ ,  $\mathbf{x}_a \in \mathbb{R}^{k \times L}$ , and  $\mathbf{s} \in \mathbb{R}^{D_s}$ , representing the prosody, content, and acoustic tokens, and the speaker embedding, respectively. Here,  $m$ ,  $n$ , and  $k$  denote the number of residual vector quantization (RVQ) codebooks for prosody, content, and acoustic representations, respectively, each with a vocabulary size of  $v$ .  $L$  is the token sequence length, and  $D_s$  is the speaker embedding dimension.

**Text Input.** Given a text transcript  $\mathbf{T}$ , we use a grapheme-to-phoneme converter [42] to obtain the corresponding phoneme sequence, which is mapped into a sequence of tokens  $\mathbf{P} = (\mathbf{P}_1, \mathbf{P}_2, \dots, \mathbf{P}_N)$  consisting of  $N$  tokens. A phoneme encoder then transforms  $\mathbf{P}$  into a sequence of embeddings  $\mathbf{p} = (\mathbf{p}_1, \mathbf{p}_2, \dots, \mathbf{p}_N) \in \mathbb{R}^{N \times D}$ , where  $D$  denotes the hidden dimension.

**Video Input.** Given a silent video  $\mathbf{V}$ , we follow the extraction pipeline in [12] to obtain the face-cropped video  $\mathbf{V}_{\text{face}}$  and lips-cropped video  $\mathbf{V}_{\text{lip}}$  and their corresponding face feature embeddings  $\mathbf{v}_{\text{face}} \in \mathbb{R}^{F \times D_f}$  and lip feature embeddings  $\mathbf{v}_{\text{lip}} \in \mathbb{R}^{F \times D_l}$ . Here,  $F$  is the number of frames, and  $D_f$  and  $D_l$  denote the face and lip feature dimensions, respectively. Since these extracted features exist in different representation spaces, we apply a 1D convolution to map them into a shared space:  $\mathbf{v}_{\text{face}} \in \mathbb{R}^{F \times D}$  and  $\mathbf{v}_{\text{lip}} \in \mathbb{R}^{F \times D}$ .

#### 3.3. Zero-shot TTS Pre-training

This stage aims to generate high-quality speech with natural prosody and expressive characteristics. To achieve this, we follow the zero-shot TTS setting, which aims to synthesize speech that faithfully reproduces the speech attributes of unseen speakers using only a few seconds of their reference speech. Let  $\mathbf{S}_r$  denote the reference speech. Our objective is to build a framework that synthesizes  $\tilde{\mathbf{S}}$  by generating prosody  $\tilde{\mathbf{x}}_p$ , content  $\tilde{\mathbf{x}}_c$ , and acoustic  $\tilde{\mathbf{x}}_a$  discrete token sequences conditioned on  $\mathbf{S}_r$  and  $\mathbf{T}$ . The key components of this stage are described below.

**Content Modeling.** As shown in Figure 2, we model the content attribute using a simple deterministic architecture (Teacher box). The phoneme sequence  $\mathbf{p}$  is processed to predict  $n$  representations for each residual codebook of the content tokens. These representations are then used to produce a content latent representation  $\tilde{\mathbf{h}}_c$  and a content probability distribution employed to predict the content tokens  $\tilde{\mathbf{x}}_c$ .

**Discrete Flow-based Prosody-Acoustic.** For prosody and acoustic attributes, we design a discrete flow-matching framework to model their joint distribution. As illustrated in Figure 2b, the denoiser outputs the joint prosody-acoustic distribution, represented as a probabilistic velocity field within the discrete flow matching process. Our denoiser is built upon a Diffusion Transformer (DiT) [43], which takes the current denoising target  $\mathbf{x}_t$ , obtained by concatenating the masked prosody and acoustic token sequences, as input. It is conditioned on the content latent representation  $\tilde{\mathbf{h}}_c$ , prosody tokens, acoustic tokens, and a speaker embedding extracted from  $\mathbf{S}_r$ , serving as contextual conditioning to predict features in  $\mathbb{R}^{(m+k) \times L \times v}$  that represent the posterior distributions for prosody and acoustic tokens. This design enables the model to simultaneously generate tokens that capture expressive prosody  $\tilde{\mathbf{x}}_p$  and realistic acoustic characteristics  $\tilde{\mathbf{x}}_a$ , remaining consistent with the speaker’s vocal

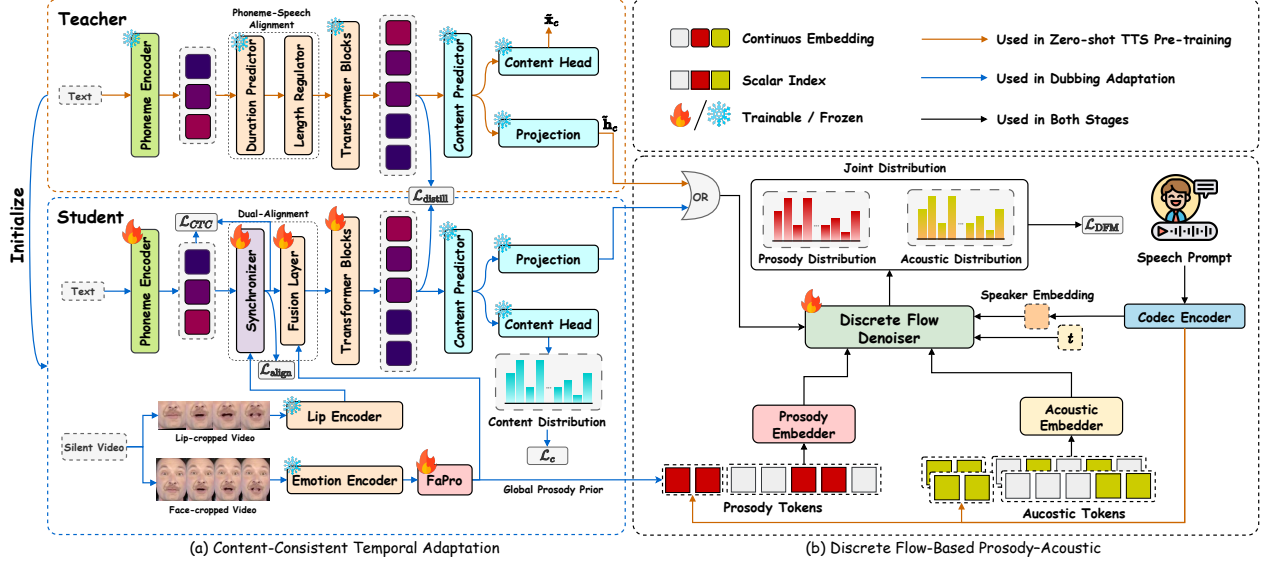


Figure 2. Pipeline of the proposed DiFlowDubber. Our framework comprises a two-stage pipeline. The first stage performs zero-shot TTS pre-training, where a simple deterministic content modeling architecture efficiently captures linguistic structure (orange dashed box). For prosody and acoustic attributes, we adopt the (b) *Discrete Flow-Based Prosody-Acoustic (DFPA)* module to model expressive prosodic variations and realistic acoustic diversity from the corpus. In the second stage, the model is adapted to V2C task. The (a) *Content-Consistent Temporal Adaptation (CCTA)* module transfers consistent content knowledge from the TTS domain and generates temporally aligned content representations, while the *FaPro* module extracts a global prosody prior from facial expression cues. The DFPA module then models the joint distribution of prosody and acoustic tokens conditioned on the prosody prior and latent content representations.

identity. The objective of the discrete flow matching process is to learn a probabilistic denoiser  $p(\mathbf{x}_1|\mathbf{x}_t)$  that reconstructs masked tokens under varying masking ratios. Formally, the model is optimized to minimize the cross-entropy loss:

$$\mathcal{L}_{DFM} = - \sum_{i \in \mathcal{T}} \mathbb{E}_{t \sim \mathcal{U}[0,1], (\mathbf{x}_0, \mathbf{x}_1), \mathbf{x}_t} [\log p_{1|t}(\mathbf{x}_1^i | \mathbf{x}_t, \mathbf{c}; \theta)], \quad (1)$$

where  $p_{1|t}(\cdot | \mathbf{x}_t, \mathbf{c}; \theta)$  denotes the posterior distribution of  $\mathbf{x}_1$  given the partially corrupted sequence  $\mathbf{x}_t$ , conditioning inputs  $\mathbf{c}$ , and  $\theta$  represents the parameters of the discrete flow matching prediction network. Here,  $\mathcal{T} = \{1, \dots, (m+k)L\}$  represents the index set of token positions,  $\mathbf{x}_t \sim p_t(\mathbf{x} | \mathbf{x}_0, \mathbf{x}_1)$  is sampled from the mixture path, and  $\mathbf{x}_0 \sim p$ ,  $\mathbf{x}_1 \sim q$  denote the source and target distributions, respectively.

Once trained, this TTS model serves as a teacher in our dubbing framework. Its pre-learned representations of pronunciation, prosody, and acoustic consistency are transferred to the video-driven dubbing stage, providing strong initialization for naturalness, pronunciation accuracy, and expressive speech generation. We encourage readers refer to the Supplementary Material for detailed architecture and training configurations of this stage.

### 3.4. Video Dubbing Adaptation

In this section, we describe how the pre-trained TTS framework is adapted for video dubbing, detailing the key components of the process.

#### 3.4.1. Face-to-Prosody Mapper

The FaPro is designed to bridge facial expressions and prosodic information in speech. In video dubbing, it is crucial that facial expressions primarily determine the prosody of the dubbed speech. Using this strong correlation, we develop FaPro to generate prosodic latent representations of speech directly from facial expressions. We first process the facial features  $\mathbf{v}_{\text{face}}$  using an upsampling layer, implemented as a learnable interpolation-convolution module, to expand the video sequence length to match that of the speech. Next, a ConvNeXt V2 [59] blocks are applied to enhance the temporal modeling capability of the resulting representations. Finally, a prosody predictor composed of  $m$  Feed-Forward Transformer (FFT) layers iteratively extracts representations for each residual codebook of prosody tokens, where each layer models dependencies conditioned on the outputs of the previous layers. We denote the resulting prosody prior representation as:  $\tilde{\mathbf{z}}_p = \text{FaPro}(\mathbf{v}_{\text{face}}) \in \mathbb{R}^{m \times L \times D}$ .

#### 3.4.2. Synchronizer

To effectively bridge the modality gap between text, video, and speech, we propose a *Synchronizer* module. It enhances video-speech alignment through the dual-alignment mechanism: video-text alignment, and speech-text alignment, which together enforce robust cross-modal synchronization. In the following, we detail the key elements of this module.

**Video-Text Alignment.** Leveraging the strong correlation

between lip movements and phonemes, we capture cross-modal interactions using transformer blocks equipped with cross-attention, where lip features  $\mathbf{v}_{\text{lip}}$  serve as queries and phoneme features  $\mathbf{p}$  as keys and values. From the final transformer block, we obtain hidden states  $\mathbf{h}_{\text{vt}} \in \mathbb{R}^{F \times D}$ , and an attention map  $\mathcal{A}_{\text{VT}} \in \mathbb{R}^{F \times N}$ . To explicitly enforce alignment, we apply a contrastive loss to the attention map  $\mathcal{A}_{\text{VT}}$ . The durations of the phonemes are obtained from the Montreal Forced Aligner (MFA) [37], converted into frame spans via the video frame rate, and used to construct a binary alignment matrix  $\mathcal{M}_{\text{VT}} \in \mathbb{R}^{F \times N}$ . Each entry  $m_{ij}$  indicates whether the  $i$ -th video frame corresponds to the  $j$ -th phoneme. The alignment loss is defined as:

$$\mathcal{L}_{\text{VT}}^{(i,j)} = -\log \frac{\sum_{i=1}^F \exp(m_{ij} \cdot a_{ij}) / \tau}{\sum_{i=1}^F \exp(a_{ij})} - \log \frac{\sum_{j=1}^N \exp(m_{ij} \cdot a_{ij}) / \tau}{\sum_{j=1}^N \exp(a_{ij})}, \quad (2)$$

where  $a_{ij}$  denotes the attention score between the  $i$ -th frame and the  $j$ -th phoneme, and  $\tau$  is temperature coefficient.

**Duration-Based Regulation.** We retain textual information by directly utilizing the attention weights obtained from Equation (2). Through *Monotonic Alignment Search* (MAS) [31], these weights are converted into phoneme-to-frame durations, allowing each phoneme embedding to be duplicated according to its assigned span. The resulting expanded sequence is then projected through a learnable transformation and added to the cross-modal hidden states  $\mathbf{h}_{\text{vt}}$ . We further upsample the resulting representation using a learnable interpolation-convolution module, expanding the sequence length to match the length of the speech features and projecting it into the latent speech space:

$$\mathbf{h}_s = \text{Upsample}(\mathbf{h}_{\text{vt}} + \text{Proj}(\text{MAS}(\mathbf{p}))) \in \mathbb{R}^{L \times D}. \quad (3)$$

**Speech-Text Alignment.** Although the previous step aligns video and text modalities, minor misalignments can still occur after upsampling. To refine synchronization, we introduce an additional contrastive alignment between the phoneme embeddings and the speech representations. Similar to the video-text alignment, transformer blocks with cross-attention are employed, where the speech features  $\mathbf{h}_s$  from Equation (3) serve as queries and the phoneme embeddings  $\mathbf{p}$  act as keys and values. From the final transformer block, we obtain hidden states  $\mathbf{h}_{\text{st}} \in \mathbb{R}^{L \times D}$  and an attention map  $\mathcal{A}_{\text{ST}} \in \mathbb{R}^{L \times N}$ . A binary alignment matrix  $\mathcal{M}_{\text{ST}} \in \mathbb{R}^{L \times N}$  is constructed analogously to  $\mathcal{M}_{\text{VT}}$  by converting the phoneme durations into speech-token spans according to the sampling rate. The phoneme-speech contrastive loss is defined as:

$$\mathcal{L}_{\text{ST}}^{(i,j)} = -\log \frac{\sum_{i=1}^L \exp(m_{ij} \cdot a_{ij}) / \tau}{\sum_{i=1}^L \exp(a_{ij})} - \log \frac{\sum_{j=1}^N \exp(m_{ij} \cdot a_{ij}) / \tau}{\sum_{j=1}^N \exp(a_{ij})}, \quad (4)$$

where  $a_{ij}$  denotes the attention score between the  $i$ -th speech token and the  $j$ -th phoneme, and  $\tau$  is temperature coefficient.

**Refinement.** Finally, the representation  $\mathbf{h}_{\text{st}}$  is refined with a ConvNeXt V2 [59] blocks, which offers strong temporal

modeling capabilities for speech-related tasks. The resulting aligned representation, denoted as  $\mathbf{h}_{\text{sync}} \in \mathbb{R}^{L \times D}$ , captures both the implicit alignment between video and speech, as well as the explicit alignments between video-text and speech-text pairs.

### 3.4.3. Content-Consistent Temporal Adaptation

CCTA facilitates the transfer of semantic content knowledge from the TTS domain and aligns it with the video to ensure temporal synchronization while preserving semantic consistency. To achieve this, we adopt the content modeling architecture and initialize its weights from the pre-trained TTS model described in Section 3.3. During adaptation, we freeze the *Projection and Content Head* and replace the duration prediction mechanism used in the TTS model with the Synchronizer module, as detailed in Section 3.4.2.

To ensure semantic and linguistic consistency, we impose a distillation constraint between the teacher (TTS) model and the student (video dubbing) model. The distillation loss enforces feature alignment by ensuring consistency between intermediate representations before they are passed to the content predictor. Specifically, we first fuse the global prosody representation  $\tilde{\mathbf{z}}_p$  with the residual content information  $\mathbf{h}_{\text{sync}}$ . The integration is performed through a fusion layer composed of channel-wise concatenation followed by linear transformations. This simple yet effective mechanism leverages the inherent alignment between prosodic and linguistic features. The resulting fused representation is then passed through transformer blocks denoted as  $\mathbf{z}_s \in \mathbb{R}^{L \times D}$  for the student feature. Similarly, we extract the corresponding representation from the teacher model before the content predictor, denoted as  $\mathbf{z}_t \in \mathbb{R}^{L' \times D}$ , where  $L'$  represents the temporal length of the teacher module. To align these feature spaces, we employ a cosine similarity-based distillation loss:

$$\mathcal{L}_{\text{distill}} = \frac{1}{B} \sum_{i=1}^B \left[ 1 - \cos(\phi(\mathbf{z}_t^{(i)}), \phi(\mathbf{z}_s^{(i)})) \right], \quad (5)$$

where  $\phi(\cdot)$  denotes the average pooling function, and  $B$  is the batch size. Finally, a content predictor, sharing the same architecture as the prosody predictor in the FaPro module, iteratively extracts  $n$  representations for each residual codebook of content tokens, denoted as  $\mathbf{h}_{\text{p2c}}$ , and passes them through a shared multi-layer perceptron (MLP) head to predict logits for each residual codebook, optimized using a cross-entropy (CE) loss:

$$\mathcal{L}_c = \text{CE}(\mathbf{x}_c, \text{MLP}(\mathbf{h}_{\text{p2c}})), \quad (6)$$

where  $\mathbf{x}_c$  denotes the target content sequence. Simultaneously, a projection layer produces a latent representation  $\hat{\mathbf{h}}_{\text{p2c}} = \text{Proj}(\mathbf{h}_{\text{p2c}}) \in \mathbb{R}^{n \times L \times D}$ , which captures the prosody-to-content correlation. This representation provides contextual guidance for modeling the subsequent speech attributes.

### 3.4.4. Discrete Flow-based Prosody-Acoustic Adaptation

To effectively inherit the capability DFPA module in capturing expressive prosody and realistic acoustic characteristics learned from large-scale TTS pre-training, we initialize the denoiser with the pre-trained weights and fine-tune it with several conditioning context modifications. In particular, the global prosody prior  $\tilde{\mathbf{z}}_p$  and the prosody-to-content correlation cues  $\tilde{\mathbf{h}}_{p2c}$  are incorporated as control signals, enabling DFPA to produce diverse yet globally coherent prosody tokens together with acoustic tokens. We elaborate on the construction of the conditioning context  $\mathbf{c}$  and describe how it is integrated into our framework.

**Contextual Modeling.** Given the current denoising target token sequences  $\mathbf{x}_t$ , which are obtained by concatenating the *prosody* token sequences  $\mathbf{x}_t^p$  and the *acoustic* token sequences  $\mathbf{x}_t^a$ , we first apply dedicated embedders to encode them into latent representations:  $\mathbf{e}_t^p = E_p(\mathbf{x}_t^p) \in \mathbb{R}^{m \times L \times D}$ ,  $\mathbf{e}_t^a = E_a(\mathbf{x}_t^a) \in \mathbb{R}^{k \times L \times D}$ . We then integrate the  $\tilde{\mathbf{h}}_{p2c}$  obtained from CCTA stage by concatenation to form the complete set of attributes, including prosody, content, and acoustic representations:  $\mathbf{e}_t = \mathbf{e}_t^p \oplus \tilde{\mathbf{h}}_{p2c} \oplus \mathbf{e}_t^a \in \mathbb{R}^{(m+n+k) \times L \times D}$ , where  $\oplus$  represents channel-wise concatenation. We then construct a conditioning representation  $\mathbf{e}_{\text{cond}} \in \mathbb{R}^{(m+n+k) \times L \times D}$ , where  $\tilde{\mathbf{z}}_p$  serves as the conditioning signal to promote diverse and expressive prosody generation. For the remaining components, zero embeddings are concatenated to maintain consistency across all quantizer streams. Finally, this process yields the complete context representation:  $\mathbf{e} = \mathbf{e}_{\text{cond}} \oplus \mathbf{e}_t \in \mathbb{R}^{(m+n+k) \times 2L \times D}$ . This embedding is fed into the denoiser, which predicts features in  $\mathbb{R}^{(m+k) \times L \times v}$  that represent the posterior distributions of the prosody and acoustic tokens, as described in Section 3.3.

### 3.5. Training Objectives

The total loss function  $\mathcal{L}_{\text{total}}$  integrates all objectives introduced in Equations (2), (4), (6), (5), and (1). In addition, following prior works [8, 9, 14], we introduce a auxiliary Connectionist Temporal Classification (CTC) loss to encourage the output of the *Synchronizer* module,  $\mathbf{h}_{\text{sync}}$ , to retain richer linguistic information. The total loss is defined as:

$$\mathcal{L}_{\text{total}} = \mathcal{L}_{\text{align}} + \lambda_1 \mathcal{L}_c + \lambda_2 \mathcal{L}_{\text{CTC}} + \lambda_3 \mathcal{L}_{\text{distill}} + \lambda_4 \mathcal{L}_{\text{DFM}}, \quad (7)$$

where  $\mathcal{L}_{\text{align}} = \lambda_5 \mathcal{L}_{\text{VT}} + \lambda_6 \mathcal{L}_{\text{ST}}$  and  $\lambda_1 - \lambda_6$  are weighting coefficients that balance the contribution of each term.

## 4. Experiments

### 4.1. Experimental Setup

**Datasets.** For zero-shot TTS pre-training, we use the **LibriTTS** [62]. In the video dubbing adaptation stage, our model is trained and evaluated on the **Chem** [25] and **GRID**

[15] datasets. Additional details are provided in the *Dataset Details* section of the Supplementary Material.

**Evaluation Metrics.** We employ comprehensive **objective metrics** to evaluate the synthesized speech. To assess temporal alignment between synthesized speech and visual content, we adopt Lip-Sync Error Confidence (LSE-C) and Lip-Sync Error Distance (LSE-D), computed using embeddings extracted from a pretrained SyncNet model [11]. For speech quality evaluation, we measure pronunciation accuracy using Word Error Rate (WER), computed with Whisper-V3 [47] as the automatic speech recognition system. Additionally, we use Speaker Encoder Cosine Similarity (SECS), following [13, 64], to quantify speaker identity consistency between the generated speech and the reference audio. Naturalness is evaluated using UTMOS [55]. To assess efficiency, we report the Real-Time Factor (RTF) under matched conditions, using a single A100 GPU and excluding video preprocessing, thereby demonstrating the computational efficiency of our discrete flow matching framework.

Along with the objective evaluations, we conduct a **subjective assessment** following the Mean Opinion Score (MOS) protocol. Specifically, we use MOS-Similarity (MOS-S) to evaluate speaker similarity. In this evaluation, 20 listeners rate 30 randomly selected synthesized speech samples on a scale from 1 to 5 based on their perceived similarity to the reference speech.

**Implementation Details & Baselines.** Please refer to the *Implementation Details* section of the Supplementary Material for a comprehensive description. Additionally, we compare our model with previous dubbing baselines, with further information provided in the *Baselines Details* section of the Supplementary Material.

### 4.2. Main Results

**Result on the Chem dataset.** As shown in Table 1, our proposed method with 128 function evaluations (NFEs) outperforms current SOTA models across most metrics on the Chem benchmark. DiFlowDubber achieves superior results in LSE-C and LSE-D, indicating stronger synchronization and demonstrating the effectiveness of our Synchronizer in enhancing temporal alignment between linguistic content and lip movements. In terms of pronunciation accuracy, our model ranks second in Setting 1.0 and achieves the best performance in Setting 2.0. Although ProDubber attains competitive WER scores in both settings, it performs poorly in lip synchronization, as reflected by its weak LSE scores, suggesting behavior closer to a TTS system rather than a true dubbing model. For speaker similarity, DiFlowDubber offers no clear advantage over the baselines, which we attribute to the shared use of identical speaker embedding model extraction in the baseline models and during SECS computation, introducing bias in favor of those systems. To

Table 1. Performance on the *Chem* dataset under both Setting 1.0 and Setting 2.0. In the Dub 1.0 Setting, the ground truth audio is used as the reference, while in the Dub 2.0 Setting, a non-ground-truth audio sample from the same speaker within the dataset is used as the reference. The best and second-best results are shown in **bold** and underlined, respectively.

Model	Setting 1.0					Setting 2.0					
	LSE-C $\uparrow$	LSE-D $\downarrow$	WER $\downarrow$	SECS $\uparrow$	UTMOS $\uparrow$	LSE-C $\uparrow$	LSE-D $\downarrow$	WER $\downarrow$	SECS $\uparrow$	MOS-S $\uparrow$	UTMOS $\uparrow$
Ground Truth	8.12	6.59	3.85	100.00	4.18	8.12	6.59	3.85	100.00	4.34 $\pm$ 0.18	4.18
V2C-Net [2] CVPR'22	1.97	12.17	90.47	51.52	1.81	1.82	12.09	94.59	44.19	-	1.76
HPMDubbing [12] CVPR'23	7.85	7.19	16.05	85.09	2.16	3.98	9.50	29.82	73.55	-	2.01
StyleDubber [13] ACL'24	3.87	10.92	13.14	<u>87.72</u>	3.14	3.74	11.00	14.18	<u>82.07</u>	4.02 $\pm$ 0.24	3.04
Speaker2Dubber [64] ACM MM'24	3.76	10.56	16.98	74.73	3.61	3.45	11.17	18.10	69.28	3.69 $\pm$ 0.25	3.64
ProDubber [65] CVPR'25	2.58	12.54	<b>9.45</b>	72.13	<u>3.85</u>	2.78	12.14	<u>11.69</u>	50.85	3.48 $\pm$ 0.26	<u>3.76</u>
EmoDubber [14] CVPR'25	<u>8.11</u>	<u>6.92</u>	11.72	<b>90.62</b>	3.82	<b>8.09</b>	<u>6.96</u>	12.81	<b>85.06</b>	4.14 $\pm$ 0.23	3.75
<b>DiFlowDubber (Ours)</b>	<b>8.31</b>	<b>6.73</b>	<u>9.65</u>	84.59	<b>4.02</b>	<b>8.37</b>	<b>6.70</b>	<b>11.12</b>	73.93	<b>4.18 <math>\pm</math> 0.18</b>	<b>4.03</b>

Table 2. Performance on the *GRID* dataset is evaluated under the same two Dub settings as in the *Chem* dataset.

Model	Setting 1.0					Setting 2.0					
	LSE-C $\uparrow$	LSE-D $\downarrow$	WER $\downarrow$	SECS $\uparrow$	UTMOS $\uparrow$	LSE-C $\uparrow$	LSE-D $\downarrow$	WER $\downarrow$	SECS $\uparrow$	MOS-S $\uparrow$	UTMOS $\uparrow$
Ground Truth	7.13	6.78	22.41	100.00	3.94	7.13	6.78	22.41	100.00	4.58 $\pm$ 0.13	3.94
V2C-Net [2] CVPR'22	5.59	9.52	47.82	80.98	2.41	5.34	9.76	49.09	71.51	-	2.40
HPMDubbing [12] CVPR'23	5.76	9.13	45.51	85.11	2.14	5.82	9.10	44.15	71.99	-	2.11
StyleDubber [13] ACL'24	6.12	9.03	18.88	<u>93.79</u>	3.73	6.09	9.08	19.58	<b>86.67</b>	3.83 $\pm$ 0.24	3.71
Speaker2Dubber [64] ACM MM'24	5.27	9.84	<u>17.07</u>	<b>94.50</b>	3.69	5.19	9.93	<u>17.42</u>	85.76	3.57 $\pm$ 0.26	3.73
ProDubber [65] CVPR'25	5.23	9.59	18.60	89.03	<u>3.87</u>	5.56	9.37	19.17	81.72	4.04 $\pm$ 0.16	<u>3.86</u>
EmoDubber [14] CVPR'25	<u>7.12</u>	<u>6.82</u>	18.53	92.22	3.83	<u>7.10</u>	<u>6.89</u>	19.75	<u>86.02</u>	4.33 $\pm$ 0.17	3.81
<b>DiFlowDubber (Ours)</b>	<b>7.32</b>	<b>6.73</b>	<b>16.79</b>	82.52	<b>3.95</b>	<b>7.28</b>	<b>6.78</b>	<b>16.21</b>	71.63	<b>4.38 <math>\pm</math> 0.18</b>	<b>3.93</b>

further verify the true perceptual similarity, we conduct an objective evaluation using the MOS-S metric under Setting 2.0. The results show that our model achieves the highest MOS-S score among the four latest baselines, highlighting that our method achieves superior speaker faithfulness where it matters most perceptually. Regarding naturalness and speech quality, as measured by UTMOS, our method also achieves SOTA results, further validating its ability to generate natural, and expressive dubbed speech.

**Result on the GRID dataset.** Table 2 reports the performance of our method with 128 NFEs compared to baseline systems. Our approach consistently achieves SOTA performance across most metrics, including synchronization (LSE-C, LSE-D), pronunciation clarity (WER), and speech quality (UTMOS), in both dubbing settings, with the exception of the SECS metric. For SECS, we assume this trend follows the same pattern as previously discussed in the Chem benchmark; nevertheless, our method achieves the highest MOS-S score. These results further confirm the effectiveness of our design choices in improving synchronization, pronunciation accuracy, and speech quality.

### 4.3. Qualitative Analysis

Figure 3 provides a qualitative comparison of the generated mel-spectrograms across different dubbing systems. Our method exhibits a strong resemblance to the ground-truth recording. The highlighted regions (in red boxes) indicate areas where different models show noticeable discrepancies,

Table 3. Ablation study results on the Chem test set.

#	Model	AVSync $\uparrow$	LSE-C $\uparrow$	LSE-D $\downarrow$	WER $\downarrow$	SECS $\uparrow$	UTMOS $\uparrow$
1	<b>Ours</b>	<b>0.721</b>	8.31	6.73	<b>9.65</b>	<b>84.59</b>	<b>4.02</b>
<i>Zero-shot TTS Pre-training</i>							
2	w/o Zero-shot TTS Pre-training	0.715	8.17	6.79	12.04	83.72	3.53
<i>Synchronizer</i>							
3	w/o ( $L_{VT} + L_{ST}$ )	0.652	8.26	6.77	17.15	84.29	3.90
4	w/o $L_{VT}$	0.681	8.36	6.71	16.57	83.94	3.87
5	w/o $L_{ST}$	0.689	8.31	6.71	12.60	84.46	3.93
<i>Content-Consistent Temporal Adaptation</i>							
6	w/o $L_{asall}$	0.713	8.33	6.70	12.62	84.23	3.97
7	w/o $L_{CTC}$	0.703	8.35	6.67	12.28	84.35	3.99
8	w/o Fuse Global Prosody Prior	0.694	8.38	6.69	10.43	79.10	3.99
<i>Facial Features</i>							
9	w/o FaPro	0.691	8.37	6.65	11.89	83.83	3.95

Table 4. Analysis of NFE in inference under the Dub 1.0 setting. #Params exclude video-related encoders.

Model	#Params	NFE	RTF $\downarrow$	LSE-C $\uparrow$	LSE-D $\downarrow$	WER $\downarrow$	SECS $\uparrow$	UTMOS $\uparrow$
ProDubber	200M	5	0.08	2.58	12.54	9.45	72.13	3.85
EmoDubber	116M	10	0.05	8.11	6.92	11.72	90.62	3.82
DiFlowDubber	250M	1	0.03	8.25	6.78	10.72	83.63	2.82
		2	0.04	8.27	6.74	10.99	83.34	2.79
		4	0.04	8.32	6.73	10.79	83.82	3.50
		8	0.05	8.29	6.73	10.28	84.50	3.85
		10	0.06	8.30	6.72	10.82	83.73	3.88
		16	0.08	8.27	6.75	11.02	83.83	3.94
		32	0.12	8.34	6.69	10.90	84.58	4.00
		64	0.22	8.32	6.70	10.79	84.07	4.03
	128	0.40	8.31	6.73	9.65	84.59	4.02	

with our results remaining most consistent with the ground truth. This demonstrates that our approach effectively preserves pitch continuity and prosodic dynamics while maintaining alignment with lip movements in the corresponding video frames. Overall, these results confirm that our model produces speech with more natural rhythm, precise synchronization, and expressive delivery that closely mirrors human dubbing performance.

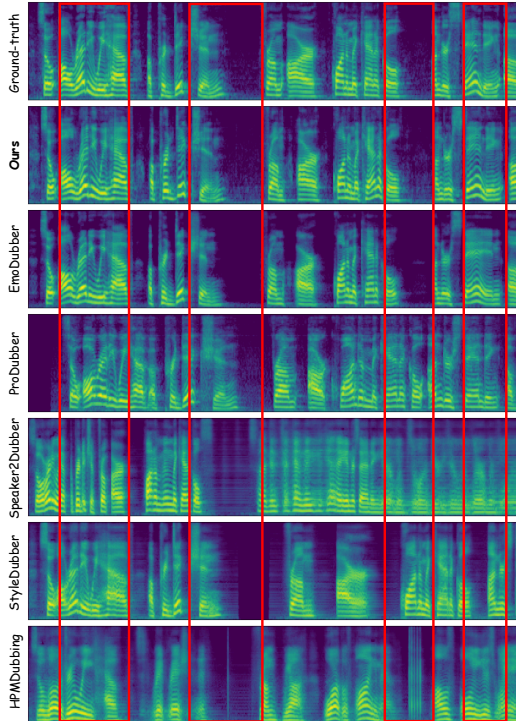


Figure 3. Mel-spectrogram visualization compared with Ground Truth (GT) speech.

#### 4.4. Ablation Study

We perform ablation studies under the Dub 1.0 setting of the Chem benchmark using 128 NFEs. To more comprehensively evaluate the contribution of the Synchronizer module, we additionally report AVSync [8] along with LSE in the standard benchmark.

**Effect of Zero-shot TTS Pre-training.** Table 3 shows that without the zero-shot TTS pre-training, the generated dubbing speech exhibits a significant reduction in naturalness and pronunciation accuracy (see row #2), demonstrating that our approach effectively inherits the expressive prosody and acoustic quality learned from large-scale TTS corpus while maintaining precise lip synchronization during dubbing.

**Effect of Synchronizer.** Table 3 shows that when the model is not constrained by cross-modal alignment (see row #3), it performs the worst in both synchronization and pronunciation accuracy, highlighting the importance of alignment constraints for performance improvement. From rows #4 and #5, we observe that using  $\mathcal{L}_{ST}$  loss is the primary driver for synchronization, significantly raising the AVSync score, while  $\mathcal{L}_{VT}$  improves both synchronization and pronunciation accuracy due to the inherent correlation between lip motion and text. Thus, combining both losses yields a more balanced and overall superior performance (see row #1).

**Effect of Content-Consistent Temporal Adaptation.** As

shown in Table 3, we observe that removing the  $\mathcal{L}_{\text{distill}}$  loss (see row #6) leads to degraded pronunciation accuracy, demonstrating the importance of effectively transferring knowledge from the TTS domain, where pronunciation is highly accurate, to the video dubbing task while maintaining temporal lip-sync alignment. When the  $\mathcal{L}_{\text{CTC}}$  loss is removed (see row #7), a similar pattern is observed, highlighting its role in facilitating more accurate alignment learning between the input text and the output of the Synchronizer. From row #8, fusing global prosody prior with content information enhances speaker similarity, indicating that face-derived global prosody encodes speaker-dependent cues. While these variants improve lip synchronization, they also introduce trade-offs in pronunciation accuracy, speaker similarity, and naturalness.

**Effect of FaPro.** Table 3 shows that removing the FaPro module (see row #9) results in consistent quality degradation across almost all metrics, confirming the importance of global prosody cues derived from facial expressions. These results indicate that FaPro effectively captures expressive facial dynamics to guide prosody modeling.

**Effect of NFE.** We conducted experiments with varying numbers of NFEs during inference on the Chem test set, as shown in Table 4. We further compare the RTF of our method with prior diffusion- and flow-based dubbing systems (ProDubber, EmoDubber). The results indicate that increasing the NFE substantially improves the UTMOS score, while other metrics remain largely stable. Performance remains consistent between 32 and 128 NFEs; notably, DiFlowDubber achieves competitive results across metrics and maintains an RTF equivalent to EmoDubber (0.05) at only 8 (RTF = 0.05) or 10 (RTF = 0.06) NFEs, despite a larger parameter count. These findings further demonstrate the advantage of the discrete flow matching framework over its counterparts based on continuous flow matching and diffusion in achieving high-quality speech with fewer sampling steps.

## 5. Conclusion

In this paper, we propose DiFlowDubber, a novel end-to-end video dubbing system that is the first to extend discrete flow matching to the field of video dubbing. Our training framework consists of two stages. First, we pre-train a zero-shot TTS model on a large-scale TTS corpus, resulting in a model that can capture linguistic information, expressive prosody and realistic acoustic characteristics. Subsequently, video adaptation is performed on the TTS model. In this stage, we introduce the Synchronizer module with a dual-alignment mechanism, achieving precise synchronization between all three modalities video, text, and speech. Both quantitative and perceptual evaluations confirm the superior performance of our method compared with prior approaches.

## References

- [1] Alexei Baevski, Yuhao Zhou, Abdelrahman Mohamed, and Michael Auli. wav2vec 2.0: A framework for self-supervised learning of speech representations. In *Advances in Neural Information Processing Systems*, pages 12449–12460. Curran Associates, Inc., 2020. 2
- [2] Qi Chen, Mingkui Tan, Yuankai Qi, Jiaqiu Zhou, Yuanqing Li, and Qi Wu. V2c: Visual voice cloning. In *2022 IEEE/CVF Conference on Computer Vision and Pattern Recognition (CVPR)*, pages 21210–21219, 2022. 7, 14
- [3] Sanyuan Chen, Shujie Liu, Long Zhou, Yanqing Liu, Xu Tan, Jinyu Li, Sheng Zhao, Yao Qian, and Furu Wei. Vall-e 2: Neural codec language models are human parity zero-shot text to speech synthesizers, 2024. 2
- [4] Sanyuan Chen, Chengyi Wang, Yu Wu, Ziqiang Zhang, Long Zhou, Shujie Liu, Zhuo Chen, Yanqing Liu, Huaming Wang, Jinyu Li, Lei He, Sheng Zhao, and Furu Wei. Neural codec language models are zero-shot text to speech synthesizers. *IEEE Transactions on Audio, Speech and Language Processing*, 33:705–718, 2025. 2
- [5] Sanyuan Chen, Chengyi Wang, Yu Wu, Ziqiang Zhang, Long Zhou, Shujie Liu, Zhuo Chen, Yanqing Liu, Huaming Wang, Jinyu Li, Lei He, Sheng Zhao, and Furu Wei. Neural codec language models are zero-shot text to speech synthesizers. *IEEE Transactions on Audio, Speech and Language Processing*, pages 1–15, 2025. 2
- [6] Yushen Chen, Zhikang Niu, Ziyang Ma, Keqi Deng, Chunhui Wang, JianZhao JianZhao, Kai Yu, and Xie Chen. F5-TTS: A fairytaler that fakes fluent and faithful speech with flow matching. In *Proceedings of the 63rd Annual Meeting of the Association for Computational Linguistics (Volume 1: Long Papers)*, pages 6255–6271, Vienna, Austria, 2025. Association for Computational Linguistics. 2
- [7] Jeongsoo Choi, Minsu Kim, and Yong Man Ro. Intelligible lip-to-speech synthesis with speech units. In *Interspeech 2023*, pages 4349–4353, 2023. 2
- [8] Jeongsoo Choi, Ji-Hoon Kim, Kim Sung-Bin, Tae-Hyun Oh, and Joon Son Chung. Alignedit: Multimodal aligned diffusion transformer for synchronized speech generation. In *Proceedings of the 33rd ACM International Conference on Multimedia*, page 10758–10767, New York, NY, USA, 2025. Association for Computing Machinery. 6, 8
- [9] Jeongsoo Choi, Zhikang Niu, Ji-Hoon Kim, Chunhui Wang, Joon Son Chung, and Xie Chen. Accelerating Diffusion-based Text-to-Speech Model Training with Dual Modality Alignment. In *Interspeech 2025*, pages 3459–3463, 2025. 6
- [10] Wei Chu and Abeer Alwan. Reducing f0 frame error of f0 tracking algorithms under noisy conditions with an unvoiced/voiced classification frontend. In *Proceedings of the 2009 IEEE International Conference on Acoustics, Speech and Signal Processing*, page 3969–3972, USA, 2009. IEEE Computer Society. 15, 16
- [11] Joon Son Chung and Andrew Senior. Out of time: automated lip sync in the wild. In *Workshop on Multi-view Lip-reading, ACCV*, 2016. 6
- [12] Gaoxiang Cong, Liang Li, Yuankai Qi, Zheng-Jun Zha, Qi Wu, Wenyu Wang, Bin Jiang, Ming-Hsuan Yang, and Qingming Huang. Learning to dub movies via hierarchical prosody models. In *Proceedings of the IEEE/CVF Conference on Computer Vision and Pattern Recognition*, pages 14687–14697, 2023. 1, 2, 3, 7, 14
- [13] Gaoxiang Cong, Yuankai Qi, Liang Li, Amin Beheshti, Zhedong Zhang, Anton Hengel, Ming-Hsuan Yang, Chenggang Yan, and Qingming Huang. StyleDubber: Towards multi-scale style learning for movie dubbing. In *Findings of the Association for Computational Linguistics ACL 2024*, pages 6767–6779, 2024. 2, 6, 7, 14
- [14] Gaoxiang Cong, Jiadong Pan, Liang Li, Yuankai Qi, Yuxin Peng, Anton van den Hengel, Jian Yang, and Qingming Huang. Emodubber: Towards high quality and emotion controllable movie dubbing. In *Proceedings of the IEEE/CVF Conference on Computer Vision and Pattern Recognition (CVPR)*, pages 15863–15873, 2025. 1, 2, 6, 7, 14
- [15] Martin Cooke, Jon Barker, Stuart Cunningham, and Xu Shao. An audio-visual corpus for speech perception and automatic speech recognition. *The Journal of the Acoustical Society of America*, 120(5):2421–2424, 2006. 6, 12, 14
- [16] Stefan Elfving, Eiji Uchibe, and Kenji Doya. Sigmoid-weighted linear units for neural network function approximation in reinforcement learning. *Neural networks*, 107: 3–11, 2018. 13
- [17] Sefik Emre Eskimez, Xiaofei Wang, Manthan Thakker, Canrun Li, Chung-Hsien Tsai, Zhen Xiao, Hemin Yang, Zirun Zhu, Min Tang, Xu Tan, et al. E2 tts: Embarrassingly easy fully non-autoregressive zero-shot tts. In *2024 IEEE Spoken Language Technology Workshop (SLT)*, pages 682–689. IEEE, 2024. 2
- [18] Qingkai Fang, Shoutao Guo, Yan Zhou, Zhengrui Ma, Shaolei Zhang, and Yang Feng. LLaMA-omni: Seamless speech interaction with large language models. In *The Thirteenth International Conference on Learning Representations*, 2025. 2
- [19] Itai Gat, Tal Remez, Neta Shaul, Felix Kreuk, Ricky T. Q. Chen, Gabriel Synnaeve, Yossi Adi, and Yaron Lipman. Discrete flow matching. In *Advances in Neural Information Processing Systems*, pages 133345–133385. Curran Associates, Inc., 2024. 2, 13
- [20] Yiwei Guo, Chenpeng Du, Ziyang Ma, Xie Chen, and Kai Yu. Voiceflow: Efficient text-to-speech with rectified flow matching. In *ICASSP 2024 - 2024 IEEE International Conference on Acoustics, Speech and Signal Processing (ICASSP)*, pages 11121–11125, 2024. 2
- [21] Bing Han, Long Zhou, Shujie Liu, Sanyuan Chen, Lingwei Meng, Yanming Qian, Yanqing Liu, Sheng Zhao, Jinyu Li, and Furu Wei. Vall-e r: Robust and efficient zero-shot text-to-speech synthesis via monotonic alignment. *arXiv preprint arXiv:2406.07855*, 2024. 2
- [22] Hongkun Hao, Long Zhou, Shujie Liu, Jinyu Li, Shujie Hu, Rui Wang, and Furu Wei. Boosting large language model for speech synthesis: An empirical study. In *ICASSP 2025 - 2025 IEEE International Conference on Acoustics, Speech and Signal Processing (ICASSP)*, pages 1–5, 2025. 2
- [23] Dan Hendrycks and Kevin Gimpel. Gaussian error linear units (gelu). *arXiv preprint arXiv:1606.08415*, 2016. 14

- [24] Nghia Huynh Nguyen Hieu, Ngoc Son Nguyen, Huynh Nguyen Dang, Thieu Vo, Truong-Son Hy, and Van Nguyen. OZSpeech: One-step zero-shot speech synthesis with learned-prior-conditioned flow matching. In *Proceedings of the 63rd Annual Meeting of the Association for Computational Linguistics (Volume 1: Long Papers)*, pages 21500–21517, Vienna, Austria, 2025. Association for Computational Linguistics. 2
- [25] Chenxu Hu, Qiao Tian, Tingle Li, Wang Yuping, Yuxuan Wang, and Hang Zhao. Neural dubber: Dubbing for videos according to scripts. In *Advances in Neural Information Processing Systems*, pages 16582–16595. Curran Associates, Inc., 2021. 6, 12, 14
- [26] A.J. Hunt and A.W. Black. Unit selection in a concatenative speech synthesis system using a large speech database. In *1996 IEEE International Conference on Acoustics, Speech, and Signal Processing Conference Proceedings*, pages 373–376 vol. 1, 1996. 2
- [27] Shengpeng Ji, Ziyue Jiang, Hanting Wang, Jialong Zuo, and Zhou Zhao. MobileSpeech: A fast and high-fidelity framework for mobile zero-shot text-to-speech. In *Proceedings of the 62nd Annual Meeting of the Association for Computational Linguistics (Volume 1: Long Papers)*, pages 13588–13600, Bangkok, Thailand, 2024. Association for Computational Linguistics. 2
- [28] Zeqian Ju, Yuancheng Wang, Kai Shen, Xu Tan, Detai Xin, Dongchao Yang, Eric Liu, Yichong Leng, Kaitao Song, Siliang Tang, Zhizheng Wu, Tao Qin, Xiangyang Li, Wei Ye, Shikun Zhang, Jiang Bian, Lei He, Jinyu Li, and Sheng Zhao. NaturalSpeech 3: Zero-shot speech synthesis with factorized codec and diffusion models. In *Proceedings of the 41st International Conference on Machine Learning*, pages 22605–22623. PMLR, 2024. 2, 3, 12, 13, 16
- [29] Zeqian Ju, Yuancheng Wang, Kai Shen, Xu Tan, Detai Xin, Dongchao Yang, Eric Liu, Yichong Leng, Kaitao Song, Siliang Tang, Zhizheng Wu, Tao Qin, Xiangyang Li, Wei Ye, Shikun Zhang, Jiang Bian, Lei He, Jinyu Li, and Sheng Zhao. NaturalSpeech 3: Zero-shot speech synthesis with factorized codec and diffusion models. In *Proceedings of the 41st International Conference on Machine Learning*, pages 22605–22623. PMLR, 2024. 2
- [30] Minki Kang, Wooseok Han, Sung Ju Hwang, and Eunho Yang. Zet-speech: Zero-shot adaptive emotion-controllable text-to-speech synthesis with diffusion and style-based models. In *Interspeech 2023*, pages 4339–4343, 2023.
- [31] Jaehyeon Kim, Sungwon Kim, Jungil Kong, and Sungroh Yoon. Glow-tts: A generative flow for text-to-speech via monotonic alignment search. In *Advances in Neural Information Processing Systems*, pages 8067–8077. Curran Associates, Inc., 2020. 2, 5
- [32] Sungwon Kim, Kevin J. Shih, Rohan Badlani, Joao Felipe Santos, Evelina Bakhturina, Mikyas T. Desta, Rafael Valle, Sungroh Yoon, and Bryan Catanzaro. P-flow: A fast and data-efficient zero-shot TTS through speech prompting. In *Thirty-seventh Conference on Neural Information Processing Systems*, 2023. 12
- [33] Matthew Le, Apoorv Vyas, Bowen Shi, Brian Karrer, Leda Sari, Rashed Moritz, Mary Williamson, Vimal Manohar, Yossi Adi, Jay Mahadeokar, and Wei-Ning Hsu. Voicebox: Text-guided multilingual universal speech generation at scale. In *Thirty-seventh Conference on Neural Information Processing Systems*, 2023.
- [34] Keon Lee, Dong Won Kim, Jaehyeon Kim, Seungjun Chung, and Jaewoong Cho. DiTTo-TTS: Diffusion transformers for scalable text-to-speech without domain-specific factors. In *The Thirteenth International Conference on Learning Representations*, 2025. 2
- [35] Ilya Loshchilov and Frank Hutter. Decoupled weight decay regularization. In *International Conference on Learning Representations*, 2019. 14
- [36] Xutai Ma, Juan Miguel Pino, James Cross, Liezl Puzon, and Jiatao Gu. Monotonic multihead attention. In *International Conference on Learning Representations*, 2020. 14
- [37] Michael McAuliffe, Michaela Socolof, Sarah Mihuc, Michael Wagner, and Morgan Sonderegger. Montreal forced aligner: Trainable text-speech alignment using kaldi. In *Interspeech 2017*, pages 498–502, 2017. 5, 12
- [38] Shivam Mehta, Ruibo Tu, Jonas Beskow, Éva Székely, and Gustav Eje Henter. Matcha-tts: A fast tts architecture with conditional flow matching. In *ICASSP 2024 - 2024 IEEE International Conference on Acoustics, Speech and Signal Processing (ICASSP)*, pages 11341–11345, 2024. 2
- [39] Lingwei Meng, Long Zhou, Shujie Liu, Sanyuan Chen, Bing Han, Shujie Hu, Yanqing Liu, Jinyu Li, Sheng Zhao, Xixin Wu, Helen M. Meng, and Furu Wei. Autoregressive speech synthesis without vector quantization. In *Proceedings of the 63rd Annual Meeting of the Association for Computational Linguistics (Volume 1: Long Papers)*, pages 1287–1300, Vienna, Austria, 2025. Association for Computational Linguistics. 2
- [40] Diganta Misra. Mish: A self regularized non-monotonic neural activation function. *arXiv preprint arXiv:1908.08681*, 2019. 14
- [41] Ngoc-Son Nguyen, Hieu-Nghia Huynh-Nguyen, Thanh V. T. Tran, Truong-Son Hy, and Van Nguyen. Diflow-tts: Discrete flow matching with factorized speech tokens for low-latency zero-shot text-to-speech, 2025. 2
- [42] Jongseok Park, Kyubyong & Kim. g2pe, 2019. 3
- [43] William Peebles and Saining Xie. Scalable diffusion models with transformers. In *Proceedings of the IEEE/CVF international conference on computer vision*, pages 4195–4205, 2023. 3, 13
- [44] Puyuan Peng, Po-Yao Huang, Shang-Wen Li, Abdelrahman Mohamed, and David Harwath. VoiceCraft: Zero-shot speech editing and text-to-speech in the wild. In *Proceedings of the 62nd Annual Meeting of the Association for Computational Linguistics (Volume 1: Long Papers)*, pages 12442–12462, Bangkok, Thailand, 2024. Association for Computational Linguistics. 2
- [45] Long-Khanh Pham, Thanh V. T. Tran, Minh-Tan Pham, and Van Nguyen. RESOUND: Speech Reconstruction from Silent Videos via Acoustic-Semantic Decomposed Modeling. In *Interspeech 2025*, pages 5613–5617, 2025. 2
- [46] Adam Polyak, Yossi Adi, Jade Copet, Eugene Kharonov, Kushal Lakhotia, Wei-Ning Hsu, Abdelrahman Mohamed,

- and Emmanuel Dupoux. Speech resynthesis from discrete disentangled self-supervised representations. In *Interspeech 2021*, pages 3615–3619, 2021. 2
- [47] Alec Radford, Jong Wook Kim, Tao Xu, Greg Brockman, Christine Mcleavy, and Ilya Sutskever. Robust speech recognition via large-scale weak supervision. In *Proceedings of the 40th International Conference on Machine Learning*, pages 28492–28518. PMLR, 2023. 6
- [48] Yi Ren, Yangjun Ruan, Xu Tan, Tao Qin, Sheng Zhao, Zhou Zhao, and Tie-Yan Liu. FastSpeech: Fast, robust and controllable text to speech. In *Advances in Neural Information Processing Systems*. Curran Associates, Inc., 2019. 2
- [49] Yi Ren, Yangjun Ruan, Xu Tan, Tao Qin, Sheng Zhao, Zhou Zhao, and Tie-Yan Liu. *FastSpeech: fast, robust and controllable text to speech*. Curran Associates Inc., Red Hook, NY, USA, 2019. 12
- [50] Yi Ren, Chenxu Hu, Xu Tan, Tao Qin, Sheng Zhao, Zhou Zhao, and Tie-Yan Liu. FastSpeech 2: Fast and high-quality end-to-end text to speech. In *International Conference on Learning Representations*, 2021. 2, 12
- [51] Jonathan Shen, Ruoming Pang, Ron J. Weiss, Mike Schuster, Navdeep Jaitly, Zongheng Yang, Zhifeng Chen, Yu Zhang, Yuxuan Wang, Rj Skerrv-Ryan, Rif A. Saurous, Yannis Agiomvrgiannakis, and Yonghui Wu. Natural tts synthesis by conditioning wavenet on mel spectrogram predictions. In *2018 IEEE International Conference on Acoustics, Speech and Signal Processing (ICASSP)*, pages 4779–4783, 2018. 2
- [52] Kai Shen, Zeqian Ju, Xu Tan, Eric Liu, Yichong Leng, Lei He, Tao Qin, sheng zhao, and Jiang Bian. NaturalSpeech 2: Latent diffusion models are natural and zero-shot speech and singing synthesizers. In *The Twelfth International Conference on Learning Representations*, 2024. 2
- [53] Yakun Song, Zhuo Chen, Xiaofei Wang, Ziyang Ma, and Xie Chen. Ella-v: Stable neural codec language modeling with alignment-guided sequence reordering, 2024. 2
- [54] Jianlin Su, Murtadha Ahmed, Yu Lu, Shengfeng Pan, Wen Bo, and Yunfeng Liu. Roformer: Enhanced transformer with rotary position embedding. *Neurocomputing*, 568:127063, 2024. 13
- [55] Takaaki Saeki and Detai Xin and Wataru Nakata and Tomoki Koriyama and Shinnosuke Takamichi and Hiroshi Saruwatari. UTMOS: UTokyo-SaruLab System for VoiceMOS Challenge 2022. In *Interspeech 2022*, pages 4521–4525, 2022. 6
- [56] Xinsheng Wang, Mingqi Jiang, Ziyang Ma, Ziyu Zhang, Songxiang Liu, Linqin Li, Zheng Liang, Qixi Zheng, Rui Wang, Xiaoqin Feng, et al. Spark-tts: An efficient llm-based text-to-speech model with single-stream decoupled speech tokens. *arXiv preprint arXiv:2503.01710*, 2025. 2
- [57] Yuxuan Wang, R.J. Skerry-Ryan, Daisy Stanton, Yonghui Wu, Ron J. Weiss, Navdeep Jaitly, Zongheng Yang, Ying Xiao, Zhifeng Chen, Samy Bengio, Quoc Le, Yannis Agiomyrgianakis, Rob Clark, and Rif A. Saurous. Tacotron: Towards end-to-end speech synthesis. In *Interspeech 2017*, pages 4006–4010, 2017. 2
- [58] Yuancheng Wang, Haoyue Zhan, Liwei Liu, Ruihong Zeng, Haotian Guo, Jiachen Zheng, Qiang Zhang, Xueyao Zhang, Shunsi Zhang, and Zhizheng Wu. MaskGCT: Zero-shot text-to-speech with masked generative codec transformer. In *The Thirteenth International Conference on Learning Representations*, 2025. 2
- [59] Sanghyun Woo, Shoubhik Debnath, Ronghang Hu, Xinlei Chen, Zhuang Liu, In So Kweon, and Saining Xie. Convnext v2: Co-designing and scaling convnets with masked autoencoders. In *Proceedings of the IEEE/CVF Conference on Computer Vision and Pattern Recognition (CVPR)*, pages 16133–16142, 2023. 4, 5, 13, 14
- [60] Yochai Yemini, Aviv Shamsian, Lior Bracha, Sharon Gannot, and Ethan Fetaya. Lipvoicer: Generating speech from silent videos guided by lip reading. In *The Twelfth International Conference on Learning Representations*, 2024. 2
- [61] Takayoshi Yoshimura, Keiichi Tokuda, Takashi Masuko, Takao Kobayashi, and Tadashi Kitamura. Simultaneous modeling of spectrum, pitch and duration in hmm-based speech synthesis. In *6th European Conference on Speech Communication and Technology*, pages 2347–2350, 1999. 2
- [62] Heiga Zen, Viet Dang, Rob Clark, Yu Zhang, Ron J. Weiss, Ye Jia, Zhifeng Chen, and Yonghui Wu. Libritts: A corpus derived from librispeech for text-to-speech. In *Interspeech 2019*, pages 1526–1530, 2019. 1, 6, 12, 14
- [63] Ziqiang Zhang, Long Zhou, Chengyi Wang, Sanyuan Chen, Yu Wu, Shujie Liu, Zhuo Chen, Yanqing Liu, Huaming Wang, Jinyu Li, et al. Speak foreign languages with your own voice: Cross-lingual neural codec language modeling. *arXiv preprint arXiv:2303.03926*, 2023. 2
- [64] Zhedong Zhang, Liang Li, Gaoxiang Cong, Haibing Yin, Yuhan Gao, Chenggang Yan, Anton van den Hengel, and Yuankai Qi. From speaker to dubber: Movie dubbing with prosody and duration consistency learning. In *Proceedings of the 32nd ACM International Conference on Multimedia, MM 2024, Melbourne, VIC, Australia, 28 October 2024 - 1 November 2024*, pages 7523–7532. ACM, 2024. 1, 2, 6, 7, 14
- [65] Zhedong Zhang, Liang Li, Chenggang Yan, Chunshan Liu, Anton van den Hengel, and Yuankai Qi. Prosody-enhanced acoustic pre-training and acoustic-disentangled prosody adapting for movie dubbing. In *Proceedings of the Computer Vision and Pattern Recognition Conference (CVPR)*, pages 172–182, 2025. 1, 3, 7, 14
- [66] Jialong Zuo, Shengpeng Ji, Minghui Fang, Mingze Li, Ziyue Jiang, Xize Cheng, Xiaoda Yang, Chen Feiyang, Xinyu Duan, and Zhou Zhao. Rhythm controllable and efficient zero-shot voice conversion via shortcut flow matching. In *Proceedings of the 63rd Annual Meeting of the Association for Computational Linguistics (Volume 1: Long Papers)*, pages 16203–16217, Vienna, Austria, 2025. Association for Computational Linguistics. 13

# DiFlowDubber: Discrete Flow Matching for Automated Video Dubbing via Cross-Modal Alignment and Synchronization

## Supplementary Material

### Summary

This appendix contains additional materials for the paper “*DiFlowDubber: Discrete Flow Matching for Automated Video Dubbing via Cross-Modal Alignment and Synchronization*”. The appendix is organized as follows:

- Section A presents dataset details, including LibriTTS for zero-shot TTS pre-training and the Chem and GRID benchmarks for video dubbing.
- Section B provides implementation details, covering pre-processing, model architectures for both the zero-shot TTS pre-training stage and the video dubbing adaptation stage, as well as training configurations.
- Section C describes the baseline methods used for comparison.
- Section D reports additional qualitative results, including alignment visualizations of the *Synchronizer* and mel-spectrogram comparisons with baseline systems.
- Section E discusses the limitations of the proposed method.

### A. Dataset Details

We adopt a two-stage training process. In the zero-shot TTS pre-training stage, we train on the LibriTTS dataset, while in the video dubbing adaptation stage, we use the Chem and GRID benchmarks.

**LibriTTS.** The LibriTTS [62] is a large-scale multi-speaker English speech corpus designed for text-to-speech (TTS) research. It contains recordings from numerous speakers with diverse accents, vocal styles, and speaking rates. Each utterance is carefully segmented and aligned with its corresponding text transcript. In our work, we use 470 hours of the LibriTTS dataset as the text-speech corpus for the zero-shot TTS pre-training stage.

**Chem.** The Chem dataset [25] consists of classroom lecture videos featuring a chemistry instructor, collected from publicly available YouTube recordings [25]. It spans approximately nine hours of content and is segmented at the sentence level to facilitate precise dubbing alignment. The dataset contains 6,082 samples for training, 50 for validation, and 196 for testing.

**GRID.** The GRID corpus [15] is a standard benchmark for evaluating multi-speaker video dubbing systems. It features recordings from 33 distinct speakers, each contributing 1,000 short English utterances. All recordings were captured under controlled studio conditions with a consistent visual back-

ground. The dataset includes 32,670 training instances and 3,280 test instances.

### B. Implementation Details

#### B.1. Preprocessing

We use FCodec [28] as the audio tokenizer, detokenizer, and speaker extractor. Audio is sampled at 16 kHz and tokenized using FCodec at 80 tokens/s, while videos are sampled at 25 FPS, resulting in a fixed 5:16 length ratio between video frames and speech tokens. Each lip-cropped frame is resized to  $96 \times 96$  pixels. The numbers of quantizers are  $m = 1$  for prosody,  $n = 2$  for content, and  $k = 3$  for acoustic tokens, each with a vocabulary size of 1024. To obtain the ground-truth alignment matrices for video-text and speech-text alignment, we first extract the duration of each phoneme using the Montreal Forced Aligner (MFA) [37]. Based on these durations, we construct the video-text alignment matrix by multiplying each phoneme’s duration by the video frame rate (25 FPS) to determine the number of frames corresponding to each phoneme. Similarly, the speech-text alignment matrix is constructed by multiplying the phoneme durations by the token rate (80 tokens/s) to obtain the number of speech tokens aligned with each phoneme.

#### B.2. Model Details

##### B.2.1. Zero-shot TTS Pre-training Stage

**Content Modeling.** Following conventional duration-based alignment modules [32, 49, 50], our architecture consists of a *Phoneme Encoder*, a *Duration Predictor*, a *Length Regulator*, and *Feed-Forward Transformer* (FFT) layers. We model the content by adapting existing duration-alignment mechanisms to the discrete token modeling setting. Specifically, we employ the duration predictor from [49] to estimate the duration (i.e., the number of tokens) for each input phoneme. Each phoneme is then duplicated by the length regulator based on the predicted durations and passed through 2 FFT blocks to refine the representations. Each FFT block contains 4 attention heads, a hidden size of 256, an output dimension of 768, convolutional filter sizes of 1024 with kernel sizes [9, 1], a dropout rate of 0.2, and a maximum sequence length of 5000. After the FFT blocks, the *Content Predictor* employs two FFT blocks with the same configuration to generate two textual representations that capture progressively richer features through the stacked FFT layers. The final output consists of two branches: the first is projected through a linear layer to obtain the *final hidden state*, while the second is projected

onto the vocabulary space to produce *logits* representing the distribution of content tokens.

**Denoiser Architecture.** We use a Diffusion Transformer (DiT) [43] as the denoiser in our discrete flow matching framework. The DiT consists of 8 layers with a hidden size of 768 and 8 attention heads, and is enhanced with rotary position embeddings (RoPE) [54]. The time step is embedded using an MLP that maps it to a 768-dimensional vector, while the speaker embedding, originally of dimension 256, is linearly projected to the same 768-dimensional space. The global conditioning vector is then formed by summing the resulting time and speaker embeddings, which are used to condition the adaptive layer normalization (AdaLN) layers. We employ a long skip connection from the input to the output of the final Transformer block. The final prediction stage performs a non-affine layer normalization followed by AdaLN modulation and a linear projection. The global conditioning vector is processed through a SiLU-activated [16] MLP to generate shift and scale parameters that modulate the normalized hidden states. The final linear projection produces an output of  $(1+3) \times 768$  dimensions, corresponding to one prosody quantizer and three acoustic quantizers.

**Contextual Modeling.** We describe the construction of the input to the *Denoiser*. The input consists of two parts: the conditioning input, denoted as  $\mathbf{e}_{\text{cond}}$ , and the current denoising target,  $\mathbf{e}_t$ .

For  $\mathbf{e}_{\text{cond}}$ , given a reference speech sample, we use FA-Codec [28] to extract discrete speech tokens along with a speaker embedding, yielding  $\tilde{\mathbf{x}}^p \in \mathbb{R}^{m \times L'}$ ,  $\tilde{\mathbf{x}}^c \in \mathbb{R}^{n \times L'}$ ,  $\tilde{\mathbf{x}}^a \in \mathbb{R}^{k \times L'}$ , and  $\mathbf{s} \in \mathbb{R}^{D_s}$ , representing the prosody, content, and acoustic tokens, and the speaker embedding, respectively. Here,  $m$ ,  $n$ , and  $k$  denote the number of residual vector quantization (RVQ) codebooks for prosody, content, and acoustic representations, each with a vocabulary size of  $v$ .  $L'$  is the token sequence length, and  $D_s$  is the speaker embedding dimension. We pass  $\tilde{\mathbf{x}}_p$  and  $\tilde{\mathbf{x}}_a$  to dedicated embedders to encode them into latent representations  $\tilde{\mathbf{e}}_p \in \mathbb{R}^{m \times L' \times D}$  and  $\tilde{\mathbf{e}}_a \in \mathbb{R}^{k \times L' \times D}$ . In the zero-shot TTS setting, which aims to mimic the speaker style of the reference speech, we omit the content tokens  $\tilde{\mathbf{x}}_c$  and replace them with a zero embedding  $\tilde{\mathbf{e}}_{\text{zeros}} \in \mathbb{R}^{n \times L' \times D}$ . The final conditioning vector is defined as  $\mathbf{e}_{\text{cond}} = \tilde{\mathbf{e}}_p \oplus \tilde{\mathbf{e}}_{\text{zeros}} \oplus \tilde{\mathbf{e}}_a$ , where  $\mathbf{e}_{\text{cond}} \in \mathbb{R}^{(m+n+k) \times L' \times D}$ , and  $\oplus$  denotes the concatenation operation.

For  $\mathbf{e}_t$ , given the current denoising target tokens  $\mathbf{x}_t = \mathbf{x}_t^p \oplus \mathbf{x}_t^a$ , we feed  $\mathbf{x}_t^p \in \mathbb{R}^{m \times L}$  and  $\mathbf{x}_t^a \in \mathbb{R}^{k \times L}$  into the same dedicated embedders to obtain latent representations  $\mathbf{e}_t^p \in \mathbb{R}^{m \times L \times D}$  and  $\mathbf{e}_t^a \in \mathbb{R}^{k \times L \times D}$ . Since speech rhythm also depends on linguistic content [66], we incorporate the content information from the *final hidden state* of the content modeling module, denoted as  $\mathbf{e}_c$ . The final denoising target is then defined as  $\mathbf{e}_t = \mathbf{e}_t^p \oplus \mathbf{e}_c \oplus \mathbf{e}_t^a$ , where

$$\mathbf{e}_t \in \mathbb{R}^{(m+n+k) \times L \times D}.$$

Finally, the complete input to the *Denoiser* is constructed by concatenating  $\mathbf{e}_{\text{cond}}$  and  $\mathbf{e}_t$  along the temporal dimension:  $\mathbf{e} = \mathbf{e}_{\text{cond}} \oplus \mathbf{e}_t$ , where  $\mathbf{e} \in \mathbb{R}^{(m+n+k) \times (L'+L) \times D}$ . The resulting tensor  $\mathbf{e}$  is then permuted to shape  $\mathbb{R}^{(L'+L) \times (m+n+k) \times D}$  and projected to  $\mathbb{R}^{(L'+L) \times D}$  before being fed into the *Denoiser*.

**Discrete Flow Matching Overview.** The objective of Discrete Flow Matching (DFM) is to transform source samples  $\mathbf{x}_0 \sim p$  into target samples  $\mathbf{x}_1 \sim q$ . In our formulation, the source distribution corresponds to all-mask tokens [MASK], while the target distribution  $\mathbf{x}_1 = \mathbf{x}_1^p \oplus \mathbf{x}_1^a$  is factorized into prosodic  $\mathbf{x}_1^p$  and acoustic  $\mathbf{x}_1^a$  components, enabling structured joint learning. Following [19], we employ a monotonic scheduler  $\kappa_t \in [0, 1]$  with boundary conditions  $\kappa_0 = 0$  and  $\kappa_1 = 1$ , where  $t \in [0, 1]$  denotes continuous time. In our implementation, we set  $\kappa_t = t^2$ . This scheduler progressively interpolates between the source and target distributions, smoothly transitioning from  $\mathbf{x}_0$  to  $\mathbf{x}_1$  as  $\kappa_t$  increases. We then construct a conditional probability path, referred to as the *mixture path*, which linearly interpolates between the source and target distributions:  $p_t(\mathbf{x}^i | \mathbf{x}_0, \mathbf{x}_1) = (1 - \kappa_t) p_0(\mathbf{x}^i | \mathbf{x}_0) + \kappa_t p_1(\mathbf{x}^i | \mathbf{x}_1)$ . This path defines an evolution of discrete states governed by a probability velocity field  $\mathbf{u}_t$ , expressed as:

$$\mathbf{u}_t^i(\mathbf{x}^i, \mathbf{x}_t) = \frac{\dot{\kappa}_t}{1 - \kappa_t} \left[ p_{1|t}(\mathbf{x}^i | \mathbf{x}_t, \mathbf{c}; \theta) - p_t(\mathbf{x}^i | \mathbf{x}_t) \right], \quad (8)$$

where  $\dot{\kappa}_t$  denotes the time derivative of the scheduler,  $\theta$  represents the learnable parameters of the probability denoiser, and  $p_{1|t}(\cdot | \mathbf{x}_t, \mathbf{c}; \theta)$  is the posterior distribution of  $\mathbf{x}_1$  given the partially corrupted sequence  $\mathbf{x}_t$  and the conditioning context  $\mathbf{c}$ .

**Total Loss.** The overall training objective in this stage consists of three components. The first term,  $\mathcal{L}_d$ , is optimized using mean squared error (MSE). The second term,  $\mathcal{L}_c$ , corresponds to the content modeling loss, computed as the cross-entropy between the predicted logits and the target content sequence. The third term is the discrete flow-matching loss,  $\mathcal{L}_{\text{DFM}}$ . The total loss is formulated as:

$$\mathcal{L} = \lambda_1 \mathcal{L}_d + \lambda_2 \mathcal{L}_c + \lambda_3 \mathcal{L}_{\text{DFM}}, \quad (9)$$

where  $\lambda_1 = 0.5$ ,  $\lambda_2 = 1.0$ , and  $\lambda_3 = 1.0$  are the weighting coefficients that balance the contribution of each term.

## B.2.2. Video Dubbing Adaptation Stage

**FaPro Module.** The architecture is composed of a learnable upsampling layer, a ConvNeXt-V2 [59] encoder stack, layer normalization, and a Transformer decoder. The upsampling layer applies linear interpolation followed by 4 sets of learnable convolutional transformations. Each set consists of a 1D convolution (kernel size 3, stride 1, padding 1), a group

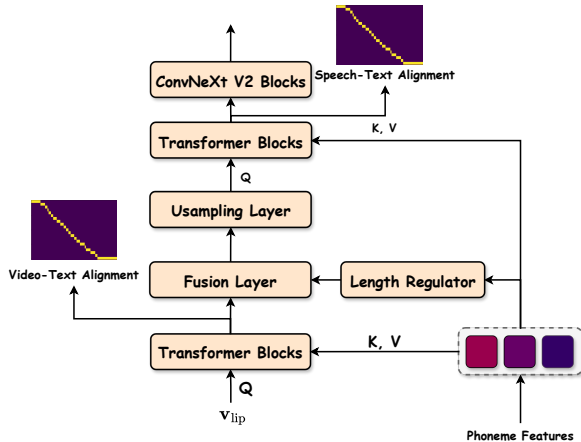


Figure 4. The detailed architecture of *Synchronizer*.

normalization layer with 1 group, and a Mish activation [40] function. A final 1D convolution projects the features to the target hidden dimension of 256. The upsampled features are then processed by a stack of 8 ConvNeXt-V2 [59] blocks, each with hidden dimension 256 and intermediate dimension 1024. Every block contains a depthwise 1D convolution with kernel size 7, followed by layer normalization and 2 linear projections. Between these projections, we apply a GELU activation [23] and a Global Response Normalization (GRN) module, which stabilizes the feature scale by normalizing the response of each channel with respect to its global L2 magnitude. A residual connection is added around each block, enabling stable and efficient learning of temporal dynamics across long facial sequences. After the ConvNeXt-V2 [59] encoder stack, a layer normalization layer is applied before forwarding the features to one Transformer decoder that serves as the *Prosody Predictor*, built on the FFT block architecture. The decoder uses 4 attention heads, a hidden dimension of 256, and a feed-forward expansion ratio of 4, and operates with a maximum sequence length of 5000.

**Synchronizer Module.** As shown in Figure 4, the module consists of 2 Transformer stacks, a learnable upsampling layer, a light fusion network, a ConvNeXt-V2 [59] encoder stack, and two layer normalization layers. We use 8 Transformer blocks for both video-text and speech-text alignment, where the attention mechanism follows a Monotonic Multi-Head Attention [36] formulation with 4 attention heads, a hidden dimension of 256, and an intermediate dimension of 1024. The learnable upsampling layer and the ConvNeXt-V2 [59] encoder stack use the same architecture and hyperparameters as those in the *FaPro* module. The light fusion network is implemented as a linear projection layer.

### B.3. Training Details

Training is conducted in 2 stages:

**Zero-shot TTS Pre-training.** We train on 470 hours of the LibriTTS dataset [62] using 4 NVIDIA A100 GPUs with a batch size of 16 for a total of 300k training steps. The learning rate is set to  $10^{-4}$  with a 10% warm-up ratio and a weight decay of 0.01, optimized using the AdamW optimizer [35]. The weighting coefficients  $\lambda_1$ ,  $\lambda_2$ , and  $\lambda_3$  are defined as in Equation 9.

**Video Dubbing Adaptation.** Training is performed on the Chem [25] and GRID [15] datasets using 4 NVIDIA A100 GPUs with batch sizes of 16 and 64, for 150 and 200 epochs, respectively. We use the AdamW optimizer [35] with a learning rate of  $10^{-3}$ , a weight decay of 0.01, and a 5% warm-up ratio. The weights for the total loss  $\mathcal{L}_{\text{total}}$  (defined in the main paper) are set to  $\lambda_1 = 1.0$ ,  $\lambda_2 = 0.1$ ,  $\lambda_3 = 0.1$ ,  $\lambda_4 = 1.0$ ,  $\lambda_5 = 0.001$ , and  $\lambda_6 = 0.001$ .

## C. Baselines Details

We compare our model with previous dubbing systems, including:

- **V2C-Net** [2] is the baseline model for the V2C task, which generates speech from text while conditioning on both reference audio and video. It fuses visual emotion cues with text and voice identity to produce speech that matches the target speaker and reflects video-driven affect.
- **HPMDubbing** [12] is a hierarchical prosody modeling framework that bridges video features (lip, face, scene) and speech prosody to improve emotional alignment and timing in video dubbing.
- **StyleDubber** [13] switches dubbing learning from the frame level to the phoneme level, using a multimodal style adaptor and phoneme-guided lip aligner to jointly model pronunciation style and visual emotion while maintaining lip-sync.
- **Speaker2Dubber** [64] is a two-stage dubbing method that first pre-trains a phoneme encoder on large-scale TTS data to learn clear pronunciation, then adapts it to video dubbing with prosody and duration consistency learning.
- **ProDubber** [65] introduces prosody-enhanced acoustic pre-training and acoustic-disentangled prosody adapting to fully leverage TTS pre-training, improving acoustic quality and prosody control in dubbing.
- **EmoDubber** [14] is an emotion-controllable dubbing architecture that uses lip-related prosody aligning, pronunciation enhancing, and a flow-based emotion controller to achieve high-quality lip sync, intelligibility, and user-specified emotion type and intensity.

## D. Additional Qualitative Results

### D.1. Alignment Visualization of Synchronizer

Figure 5 visualizes the attention maps learned by the *Synchronizer* module. The left panel shows the video-text align-

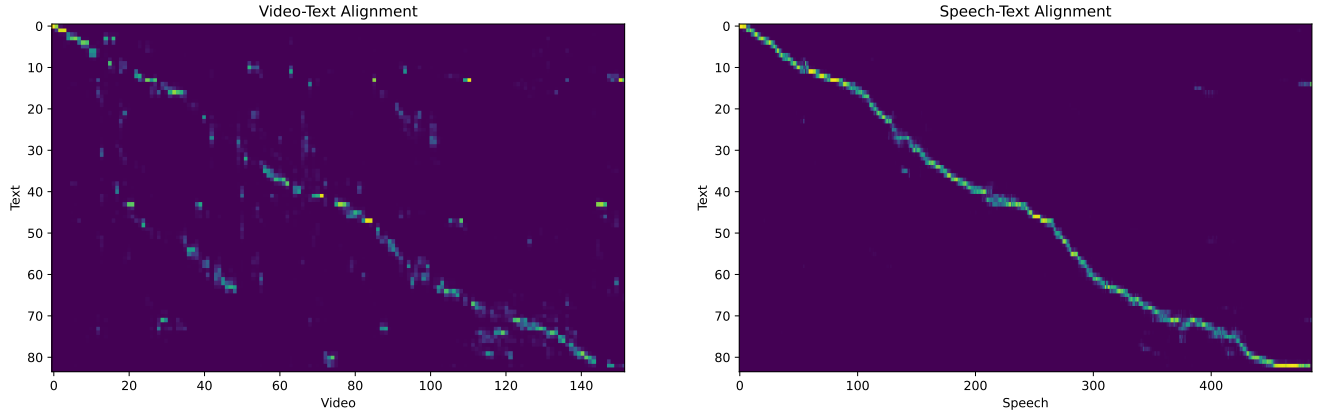


Figure 5. Alignment visualization of the *Synchronizer*. Left: Video-Text alignment matrix. Right: Speech-Text alignment matrix.

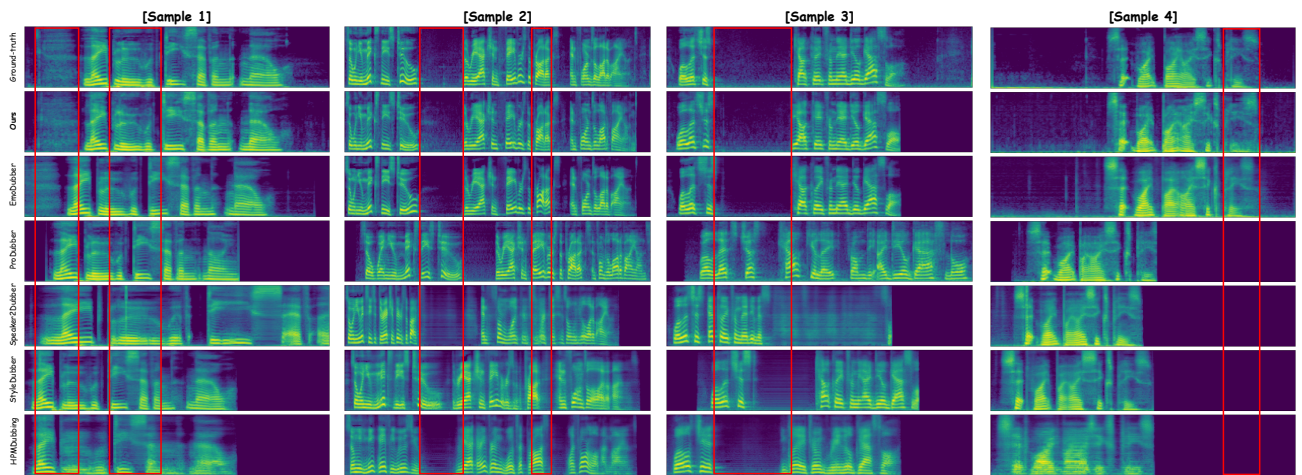


Figure 6. Qualitative comparison of mel-spectrograms. Our method produces spectra closest to the ground-truth, with clearer harmonics, cleaner pauses, and better temporal synchronization than baseline methods.

ment between lip-frame features and phoneme embeddings, while the right panel shows the speech-text alignment between discrete speech tokens and phonemes. In both cases, the attention concentrates along a clear diagonal, indicating monotonic and fine-grained temporal alignment. This confirms that the *Synchronizer* successfully learns to align visual and speech streams with the textual content, providing a reliable cross-modal bridge that underpins the strong lip synchronization and pronunciation accuracy observed in our experiments.

## D.2. Mel-spectrogram Visualization

We provide additional qualitative comparisons in Figure 6. For 4 representative samples, we visualize the mel-spectrograms of the ground-truth speech, our DiFlowDubber, and all baseline methods. The red bounding boxes highlight regions where different models exhibit noticeable differences in speech quality. Across all samples, our method produces spectra most similar to the ground-truth, preserving clear

harmonic structure and temporal dynamics. The voiced regions in our results align well with the visual boundaries, whereas baseline systems often exhibit temporal drift and over-smoothed harmonics, resulting in degraded synchronization.

## D.3. Expressive Metrics for Prosody Validation

To effectively validate that the DFPA module generates diverse yet globally consistent prosody under the guidance of the FaPro module, we conduct additional evaluations using a set of expressive prosody metrics that directly measure pitch modeling accuracy and emotional consistency:

- **Gross Pitch Error (GPE)** [10]: Measures the percentage of voiced frames where the relative error between the fundamental frequency  $F_0$  of synthesized speech and the ground truth exceeds a predefined threshold (typically 20%), indicating major pitch deviations.
- **Voicing Decision Error (VDE)** [10]: Computes the percentage of frames with incorrect voiced/unvoiced deci-

Table 5. Evaluation of prosodic expressiveness and emotional consistency on the Chem dataset (Setting 2.0).

Model	FFE↓	GPE↓	VDE↓	Emo-SIM↑
HPMDubbing	0.535	0.473	0.289	0.979
StyleDubber	0.583	0.493	0.360	0.976
Speaker2Dubber	0.639	0.519	0.408	0.979
ProDubber	0.653	0.562	0.436	0.959
EmoDubber	0.426	0.408	0.220	0.977
<b>DiFlowDubber (ours)</b>	<b>0.395</b>	<b>0.361</b>	<b>0.209</b>	<b>0.983</b>

sions relative to the reference, reflecting rhythmic consistency.

- **F0 Frame Error (FFE)** [10]: Combines GPE and VDE, representing the percentage of frames with either gross pitch error or incorrect voicing decisions, thereby summarizing overall  $F_0$  modeling accuracy.
- **Emotion Similarity (Emo-SIM)**: Measures emotional consistency by computing the cosine similarity between emotion embeddings extracted from the synthesized and reference speech using a pretrained emotion recognition model. In our experiments, we adopt the Emo2Vec model for embedding extraction.

Since the global prosody prior is derived from facial expressions, the target expressive intent is implicitly encoded in the corresponding ground-truth speech. Therefore, we use the ground-truth audio directly as the reference when computing these metrics, enabling us to measure how faithfully the synthesized speech aligns with the intended prosodic and emotional characteristics. As shown in Table 5, we conduct the evaluation under Setting 2.0 to simulate a more challenging scenario for expressive dubbing. The results show that DiFlowDubber achieves the best performance across all expressive metrics. Specifically, our model significantly reduces pitch and voicing errors compared to strong baselines like EmoDubber (0.395 vs. 0.426 FFE), while achieving the highest emotional consistency (0.983 Emo-SIM). These findings confirm that leveraging facial dynamics as a prosody prior effectively guides the DFPA module to generate speech that is both prosodically and emotionally consistent with the visual content.

## E. Limitations

Although our proposed method significantly enhances the quality of generated dubbing, it still faces certain limitations. Since the framework depends on the third-party FACodec [28], from which it inherits certain constraints. In future work, we plan to adapt our system to operate with alternative codec models. Furthermore, the current design does not fully meet expectations in voice cloning. Developing more effective approaches to mimic speaker timbre from audio in real-world video dubbing remains an open area for

<https://github.com/ddlBoJack/emotion2vec>

improvement.